IEEE Access
Multidisciplinary ⋮ Rapid Review ⋮ Open Access Journal

Received 3 October 2023, accepted 8 October 2023, date of publication 13 October 2023, date of current version 18 October 2023.

Digital Object Identifier 10.1109/ACCESS.2023.3323613

RESEARCH ARTICLE

Simulation Optimization of Collaborative Handshake Operations for Twin Overhead Shuttle Cranes in a Rail-Based Automated Container Terminal Under Demand Uncertainty

BONGGWON KANG[1], BOSUNG KIM[1], AND SOONDO HONG[2]
[1]Major in Industrial Data Science and Engineering, Department of Industrial Engineering, Pusan National University, Busan 46241, South Korea
[2]Department of Industrial Engineering, Pusan National University, Busan 46241, South Korea

Corresponding author: Soondo Hong (soondo.hong@pusan.ac.kr)

This work was supported in part by the National Research Foundation of Korea (NRF) through the Korean Government (MSIT) under Grant NRF-2020R1A2C2004320; and in part by the "Human Resources Program in Energy Technology" of the Korea Institute of Energy Technology Evaluation and Planning (KETEP), granted Financial Resource from the Ministry of Trade, Industry and Energy, South Korea, under Grant 20214000000520.

ABSTRACT A handshake operation can mitigate workload imbalance and interference between twin transporters in a material handling system. Terminal operators in a rail-based automated container terminal can employ the handshake operation to twin overhead shuttle cranes (OSs) under maritime demand uncertainty. Since a handshake location is critical to collaboration performance, terminal operators often rely on simulation experiments with a manual iterative design to determine optimal handshake locations. However, the simulation optimization is still challenging when a simulation execution is computationally expensive. This study proposes a Bayesian optimization-based approach to expedite the decision-making process. The approach infers the conditional outcomes of a simulation and actively searches optimal handshake locations. Our optimization results show that the proposed approach maximizes the collaborations between the twin OSs within fewer simulation runs. This study also provides extensive simulation analysis of the handshake locations. The experiments indicate that a handshake location has a significant influence on the required space for handshake operations and the workloads of the twin OSs.

INDEX TERMS Container terminal, handshake operation, simulation, simulation optimization.

I. INTRODUCTION

In response to growing transportation volume, material handling systems such as warehouses and container terminals have adopted twin transporter systems [3], [4], [5]. Collaboration between transporters, i.e., workers, vehicles, and cranes, in these systems is critical to performance since it can mitigate interference and workload imbalance [6]. However, improper collaboration design can lead to performance degradation due to significantly increased blocking and congestion between twin transporters. In the container terminal industry, terminal operators have sought an efficient design of collaborative operations for upcoming maritime transportation demands [7], [8].

The associate editor coordinating the review of this manuscript and approving it for publication was Jolanta Mizera-Pietraszko.

Container terminals function as a multimodal interface between the seaside for vessel berthing and the landside for container storing [9], [10]. The bottleneck in terminal operations has shifted from the seaside to the landside with the development of seaside equipment and their technologies [11]. A terminal's global competitiveness depends on shortening the lengthy turnaround times required by mega-vessels. Lee et al. [1] investigated a novel rail-based automated container terminal (RACT) to shorten the turnaround times of mega-vessels and achieve low-carbon sustainable development in the container terminal industry. Fig. 1 shows the schematic layout of a RACT.

The landside in the RACT comprises multiple overhead rails to store and transport containers. Twin overhead shuttle cranes (OSs) hanging from each overhead rail transport containers between flatcars and external trucks (ETs). The OSs

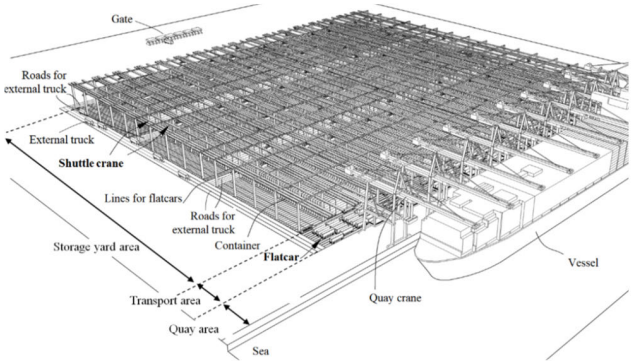

FIGURE 1. Schematic layout of a RACT [1].

cannot pass over each other, so interference between them inevitably occurs due to time-variant port operations. To mitigate interference, the terminal operators in the RACT can use a handshake operation to divide a task into two subtasks with shorter travel distances based on handshake locations. The workload is the time required to complete all tasks. Since a handshake location is critical to collaboration performance, the terminal operators aim to optimize the locations within a limited planning time.

Terminal operators have widely relied on simulation-based decision-making to enhance container terminal performance, which shows a black-box function from complex and uncertain operations [12], [13], [14]. One practical simulation optimization approach for handshake locations is a manual iterative method. In addition, many studies perform exhaustive simulation runs to identify optimal handshake locations for strategic yard operations, i.e., yard crane scheduling and storage space allocation, in container terminals [3], [7], [15]. However, due to the computational expense of a single run of a high-fidelity and large-scale simulation, it can be challenging to provide optimal locations within a limited planning time.

As operational unreliability may lead to significant changes in original plans and high adaptation costs to maritime demand uncertainty, operational reliability has become a critical factor in the container terminal industry [16]. When a terminal operator establishes operational planning for yard operations, the operator can consider demand uncertainty to achieve handshake locations with improved reliability. This study addresses a scenario-based approach to optimize the handshake locations. The approach accounts for an uncertain parameter as a finite set of deterministic scenarios based on their probabilities [17]. Since the scenario-based approach requires a corresponding increase in simulation time to the number of scenarios, we focus on the acceleration of the simulation optimization.

This study makes the following contributions: (1) we introduce a scenario-based handshake location determination model (SHLD) based on mixed-integer programming (MIP) and present a discrete-event simulation model to describe the collaborative activities between twin OSs; (2) we propose a Bayesian optimization-based decision-making for handshake locations under maritime demand uncertainty and perform a comprehensive simulation analysis of handshake locations on the collaborative operations between twin OSs.

The remainder of this paper is organized as follows: Section II reviews the literature and associated challenges. Section III discusses the handshake operations in the twin OS system and the SHLD. Section IV proposes our simulation optimization approach for determining the handshake locations under demand uncertainty. Section V provides the simulation experiments and the results. Section VI concludes with suggestions for future research.

II. LITERATURE REVIEW

Previous studies have investigated the collaborative operations of multiple cranes with predetermined handshake locations. Briskorn et al. [18], who developed a scheduling algorithm for twin cranes that could not pass each other, showed that handshake operations synchronized yard crane operations by mitigating the interference between cranes. Carlo and Martínez-Acevedo [19] identified the effectiveness of the priority rules for twin cranes in yard operations and developed a branch-and-bound algorithm to optimize the rules. Overlapping twin cranes triggered cooperative operations with a predetermined handshake location in the middle of the yard block. This approach dynamically created new branches during interference and minimized the makespan of tasks with less computational time. Chen et al. [20], who proposed an integrated scheduling model to synchronize automated guided vehicles and yard cranes with a handshake location along the crane pathway, confirmed that the proposed model obtained near-optimal solutions close to the optimal vehicle travel time. Zey et al. [3] suggested a branch-and-bound algorithm for optimal twin-crane scheduling with a dedicated handshake location. The proposed algorithm accounted for the precedence constraints in handshake operations. Zey et al. [3] also performed a simulation analysis of the handshake location on the makespan for all tasks. Han et al. [7] proposed an MIP model and a genetic algorithm to minimize the makespan of all containers with handshake operations. The experimental results indicated that the proposed algorithm provided efficient solutions with a fixed handshake location, preliminarily determined by exhaustive simulation experiments. They also suggested a prompt optimization of the handshake location for future research. Chu et al. [21] suggested an MIP model and heuristic approaches for a triple yard crane scheduling problem in two adjacent container blocks considering variant container handling time. Lee et al. [22] proposed a genetic algorithm incorporating non-interference constraints for a multiple quay crane scheduling problem. The experimental results indicated that the proposed approach yielded near-optimal solutions for both three and four quay crane cases.

Several studies have discussed optimization problems under realistic uncertainties in container terminals. Zhen [23]

proposed a scenario-based stochastic approach for optimal yard template planning under demand uncertainty in the global maritime logistics market. Gumuskaya et al. [24] investigated a two-stage stochastic procedure for optimizing periodic barge planning under container arrival uncertainty. The procedure used a decision tree to predict the uncertain factors described in their MIP model; the expected barge costs were optimized more effectively than alternative approaches. Wang et al. [25], who proposed a mixed-integer nonlinear programming model with a sample-average approximation based on dual decomposition and Lagrangian relaxation techniques, solved the container slot allocation problem under demand uncertainty. The experimental results indicated that the proposed model could achieve profit growth under demand uncertainty. Liu et al. [26] proposed a scenario-based stochastic model and its metaheuristic method for the berth allocation problem to satisfy the service level under fluctuating vessel arrival and operation times. Xiang and Liu [27] investigated a robust optimization model for integrated berth allocation with quay crane assignment under fluctuating vessel arrival times and container quantities. Applying K-means clustering to separate the uncertainty set achieved a less conservative solution. Zhen et al. [28], who developed a two-stage decision-making model and a metaheuristic approach to optimize the berth allocation problem under fluctuating vessel arrival and operation times, showed that the stochastic approaches outperformed deterministic approaches under uncertainty.

Other studies have performed simulation analyses and optimizations of container terminals, e.g., the simulation analysis of layout designs and recharging policies for a battery-powered vehicle-based container terminal [29]. Gharehgozli et al. [8] evaluated the effects of priority rules, handshake locations, and scheduling heuristics on yard operations. Yıldırım et al. [30] introduced a simulation model and an optimization method using a swarm-based artificial bee colony optimization algorithm to solve the berth allocation problem. He et al. [12] employed a genetic algorithm-based simulation optimization method to optimize decision-making for sharing internal trucks among multiple container terminals. Zeng et al. [31] developed an integrated simulation model considering the seaside and the landside of a container terminal. They proposed an MIP model and a two-level genetic algorithm to optimize dual-cycling operations. The heuristic method reduced the rehandling operations of the quay cranes. Zhou et al. [32] proposed a simulation optimization approach for solving an integrated yard allocation problem under vehicle congestion which iteratively solved an MIP model for the yard allocation problem and evaluated the time-variant vehicle traffic via simulation until the termination criteria were met. The iterative method updated the parameters of the MIP model and obtained efficient yard allocation decisions. Other studies of simulation optimization approaches accelerated simulation-based decision-making at container terminals [33], [34], [35].

Collaboration between neighboring transporters, i.e., workers, vehicles, and cranes, in various material-handling systems is essential for balancing workloads and mitigating interference. Hong [36] proposed a queuing-based analytical model to estimate the interference of downstream workers under the non-instantaneous walk times of upstream workers in a bucket brigade order-picking system. Hong [37] also performed a simulation analysis of worker speed, number of workers, and working time for collaboration between multiple workers in a bucket brigade order-picking system. Lim [38] proposed a bucket brigade protocol for cooperation between multiple workers in a production system. The experimental results indicated that the protocol reduced unproductive travel time and improved throughput by around 7%. Fan et al. [15] developed an MIP model for twin-crane scheduling with handshake operations considering the minimum distance between the cranes and space for handshake operations with a fixed handshake location. Exhaustive simulation experiments identified the effects of different handshake locations on the makespan of all tasks.

Simulation optimization approaches have gained attention with the emergence of high-fidelity simulations. Bayesian optimization (BO) has been used for optimizing an expensive black-box function based on a surrogate model estimating an objective function over candidate solutions, and an acquisition function quantifying their potentialities based on the predicted objective function. A suitable choice of surrogate model efficiently learned an objective function and reduced computing resources [39]. Candelieri et al. [40] used BO to solve scheduling problems in water distribution systems and achieved an effective solution with limited evaluations. Kang et al. [41] suggested an MIP model and a BO to optimize the collaborative operations between twin OSs given exact demand information. The experimental results indicated that the BO was beneficial when the container terminal had complex constraints difficult to formulate explicitly.

III. PROBLEM DEFINITION

In this section, we describe the detailed layout of our target RACT with container flows, the collaborative operations between twin OSs, and a scenario-based handshake location determination problem considering demand uncertainty.

A. RACT CONFIGURATIONS

Rail-based designs for enhancing throughput capacities and ensuring accurate container handling operations in container terminals have been discussed [42], [43]. OSs in a RACT travel at higher speeds on rails above container storage areas than the yard cranes used in traditional terminals. Although rail-based designs save the wasted space on aisles, mitigate interference between OSs and vehicles during travel [42], and provide routing options for vehicle travel, the RACT reduces the flexibility of OSs' movement [43]. The RACT requires a sophisticated control system to ensure safe operations based on error detection and breakdown recovery from hazards

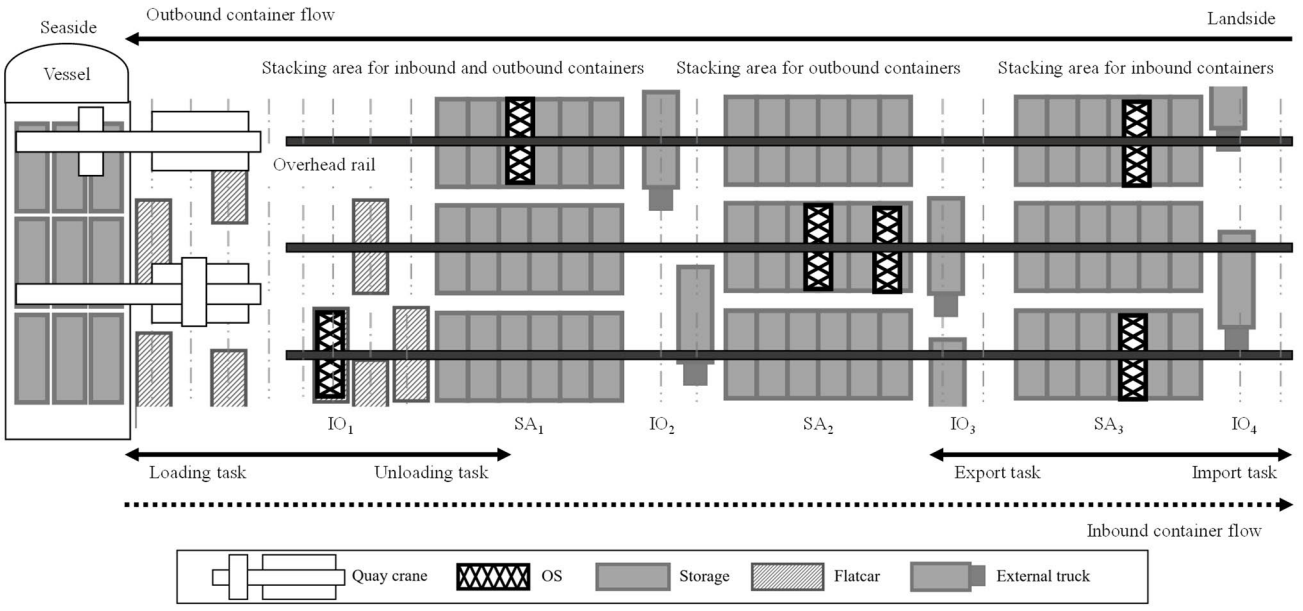

FIGURE 2. RACT configuration with container flows.

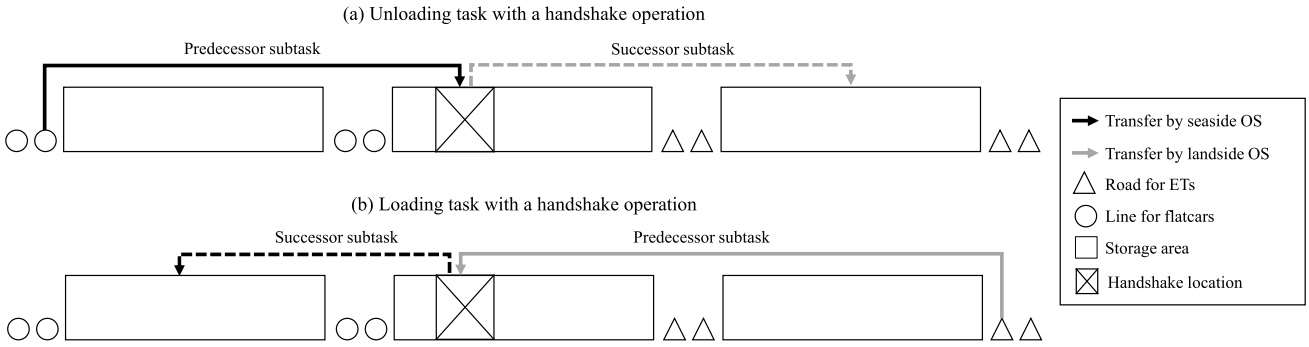

FIGURE 3. Precedent relationship between subtasks (modified from Fibrianto et al. [2]).

within the RACT, e.g., collisions between OSs and equipment breakdowns due to adverse climate conditions [44], [45].

Fig. 2 shows the RACT and its container flows, and storage assignments based on interviews with industry experts. An inbound container is unloaded from a vessel and loaded onto an ET, and an outbound container is released from an ET and loaded onto a vessel [46]. On the seaside (landside), seaside (landside) OSs deliver and pick up containers to and from flatcars (ETs). The OSs repeat four basic operations for a task: empty travel, pick-up, loaded travel, and drop-off. Export and unloading tasks distributed throughout the RACT are categorized as storage tasks, and import and loading tasks collected throughout the RACT are categorized as retrieval tasks.

There are three stacking areas in the yard storage: SA_1 for all containers, SA_2 for outbound containers, and SA_3 for inbound containers. IO_1 and IO_2 correspond to flatcars and IO_3 and IO_4 points correspond to ETs. Containers from vessels denote the unloading and loading tasks corresponding to IO_1. Transshipment containers correspond to IO_2. Containers from ETs denote the import and export tasks corresponding to IO_2, IO_3, and IO_4.

B. PRIORITY RULE AND HANDSHAKE OPERATIONS

Container terminals generally prioritize seaside crane operations because the crane continuously transports containers during peak hours, whereas landside crane operations are less frequent [18]. When the twin cranes overlap, the low-priority crane should wait until the high-priority crane finishes its current task. The low-priority crane moves from its destination to yield to the high-priority crane. A handshake operation of the RACT is to maximize the workload balance between overlapping cranes under the priority rule.

The handshake operation separates a task into two subtasks with shorter travel distances for each OS (See Fig. 3). For a handshake operation, a pair of subtasks has a precedent relationship based on the handshake location. The subtasks are identified as predecessor and successor subtasks.

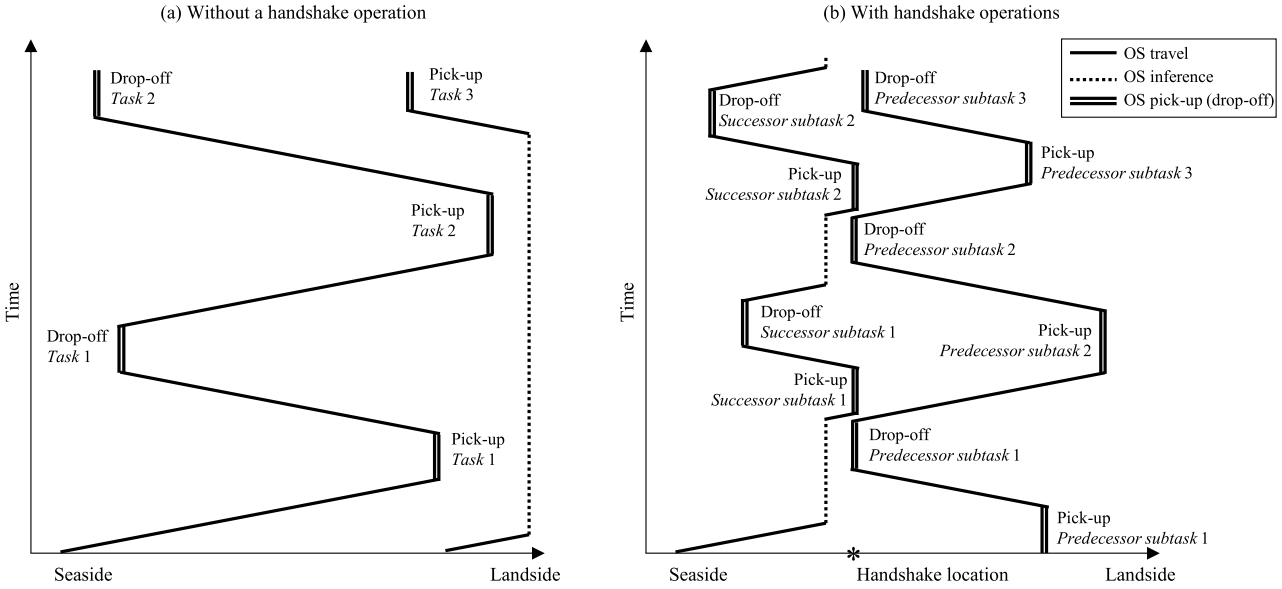

FIGURE 4. Exemplary time-space diagrams without and with handshake operations.

One OS temporarily drops a predecessor subtask at a handshake location and the other OS delivers its successor subtask from the handshake location to its destination (See Fig. 3). Fig. 4 shows the time-space diagrams with and without handshake operations. Fig. 4 (b) shows the reduced interference and enhanced workload balance between the OSs.

This study applied the handshake operation for a task crossing over the boundary between stacking areas because applying the handshake operation to a task with a shorter travel distance can decrease yard productivity owing to additional pick-up and drop-off operations. We consider two handshake locations for unloading and loading tasks based on Gharehgozli et al. [8]. The authors showed that using two handshake locations significantly improved productivity by reducing container rehandling to remove containers stacked on a target container.

C. SCENARIO-BASED HANDSHAKE LOCATION DETERMINATION MODEL (SHLD)

A scenario-based approach can describe demand uncertainty as a finite set of deterministic demands. The terminal operator can design possible scenarios with their probabilities by referring to the historical data. Consequently, the terminal operator may obtain a reliable solution for uncertain demands. We aim to minimize the maximum workload of all scenarios and solve the worst-case disturbance effect. The min-max optimization is a common approach for robust decision-making in real-world problems [47].

An MIP model provides a comprehensive understanding of the optimization problem. Field operators may easily implement mathematical models using commercial solvers, providing the flexibility to add or remove constraints to match the requirements of optimization problems in practice. The SHLD estimates the workloads of the twin OSs by multiplying the number of tasks by their central distances between nodes. It also approximates the empty travel of the twin OSs, given three assumptions: (1) the total number of empty travels equals the total number of tasks; (2) the total number of empty travels from each node equals the total number of tasks to each node; and (3) the total number of empty travels to each node equals the total number of tasks from each node. Finally, the SHLD provides the optimal handshake locations with linear constraints. We use the following indices, sets, parameters, and formulations:

Indices and sets:

N	Set of all nodes.
A	Set of stacking areas.
P	Set of I/O points.
i, j	Indices for all nodes.
T, t	Set of task types and its index.
K, k	Set of OSs and its index.
PU, u	Set of unloading handshake locations and its index.
PL, l	Set of loading handshake locations and its index.
S, s	Set of scenarios and its index.

Parameters

f_{is}^{t}	Number of tasks with type t from node i in scenario s.
UR_s	Unloading handshake operation rate in scenario s.
LR_s	Loading handshake operation rate in scenario s.
t_{ijk}	Processing time of OS k from node i to j.
ut_{ijku}	Processing time of OS k from node i to j using unloading handshake location u.
lt_{ijkl}	Processing time of OS k from node i to j using loading handshake location l.
et_{ijk}	Empty travel time of OS k from node i to j.

Decision variables

M^{max}	Maximum workload of OSs of all scenarios.
M_s	Maximum workload of OSs in scenario s.
x_u	If unloading handshake location u is used $x_u = 1$, otherwise $x_u = 0$.
x_l	If loading handshake location l is used $x_l = 1$, otherwise $x_l = 0$.
F_{ijks}	Number of non-handshake tasks of OS k from node i to j in scenario s.
U_{ijkus}	Number of tasks of OS k from node i to j with handshake location u in scenario s.
L_{ijkls}	Number of tasks of OS k from node i to j with handshake location l in scenario s.
T_{ijks}	Number of tasks of OS k from node i to j for estimating empty flows in scenario s.
E_{ijks}	Number of empty travels of OS k from node i to j.

Objective function

$$\text{(SHLD) } Minimize\ M^{max} \tag{1}$$

Constraints

$$M^{max} \geq M_s, \quad \forall s \in S, \tag{2}$$

$$M_s \geq \sum_{i\in N, j\in N} \Big(F_{ijks} \cdot t_{ijk} + E_{ijks} \cdot et_{ijk} + \sum_{u\in PU} U_{ijkus} \cdot ut_{iju} + \sum_{l\in PL} L_{ijkls} \cdot lt_{ijkl} \Big) \cdot p_s, \quad \forall k \in K, \forall s \in S, \tag{3}$$

$$F_{ijks} \geq f^U_{is} \cdot (1 - UR_s), \quad \forall i \in \{P_1\}, \forall j \in \{A_1\}, \forall k \in \{K_s\}, \forall s \in S, \tag{4}$$

$$F_{ijks} \geq f^L_{is} \cdot (1 - LR_s), \quad \forall i \in \{A_1\}, \forall j \in \{P_1\}, \forall k \in \{K_s, \forall s \in S, \tag{5}$$

$$\sum_{j\in A, k\in K} F_{ijks} \geq f^I_{is}, \quad \forall i \in P, \forall s \in S, \tag{6}$$

$$\sum_{j\in P, k\in K} F_{ijks} \geq f^O_{is}, \quad \forall i \in A, \forall s \in S, \tag{7}$$

$$U_{ijkus} \geq \sum_{w\in N} f^U_{ws} \cdot UR_s \cdot x_u, \quad \forall i \in \{P_1\}, \forall j \in \{B_u\}, \forall k \in \{K_s\}, \forall u \in PU, \forall s \in S, \tag{8}$$

$$U_{ijkus} \geq \sum_{w\in N} f^U_{ws} \cdot UR_s \cdot x_u, \quad \forall i \in \{B_u\}, \forall j \in \{A_3\}, \forall k \in \{K_l\}, \forall u \in PU, \forall s \in S, \tag{9}$$

$$L_{ijkls} \geq \sum_{w\in N} f^L_{ws} \cdot LR_s \cdot x_l, \quad \forall i \in \{A_2\}, \forall j \in \{B_l\}, \forall k \in \{K_l\}, \forall l \in PL, \forall s \in S, \tag{10}$$

$$L_{ijkls} \geq \sum_{w\in N} f^L_{ws} \cdot LR_s \cdot x_l, \quad \forall i \in \{B_l\}, \forall j \in \{P_1\}, \forall k \in \{K_s\}, \forall l \in PL, \forall s \in S, \tag{11}$$

$$\sum_{u\in PU} x_u = 1, \tag{12}$$

$$\sum_{l\in PL} x_l = 1, \tag{13}$$

$$T_{ijks} = F_{ijks}, \quad \forall i, j \in N/\{B_u, B_l\}, \forall k \in K, \forall s \in S, \tag{14}$$

$$T_{ijks} = \sum_{u\in PU} U_{ijkus}, \quad \forall i, j \in N, \forall k \in K, \forall s \in S, \tag{15}$$

$$T_{ijks} = \sum_{l\in PL} L_{ijkls}, \quad \forall i, j \in N, \forall k \in K, \forall s \in S, \tag{16}$$

$$\sum_{i\in N, j\in N} E_{ijks} = \sum_{i\in N, j\in N} T_{ijks}, \quad \forall k \in K, \forall s \in S, \tag{17}$$

$$\sum_{j\in N} E_{ijks} = \sum_{j\in N} T_{ijks}, \quad \forall i \in N, \forall k \in K, \forall s \in S, \tag{18}$$

$$\sum_{i\in N} E_{ijks} = \sum_{i\in N} T_{ijks}, \quad \forall j \in N, \forall k \in K, \forall s \in S. \tag{19}$$

The objective is to minimize the maximum workload of all scenarios. Constraints (2) and (3) update the maximum workload of the twin OSs in each scenario. Constraints (4)-(7) update an OS's workload for a task and constraints (8)-(11) calculate the workloads of both for a task separated as two subtasks (See Fig. 4). In detail, constraints (4) and (5) calculate the container flows of unloading and loading tasks without handshake operations. Constraints (6) and (7) calculate the container flows of the import and export tasks. Constraints (8) and (9) separate the unloading tasks based on the handshake locations for workload partitioning between the twin OSs, and constraints (10) and (11) separate the loading tasks based on the handshake locations for workload partitioning between the twin OSs. Constraints (12) and (13) update the handshake locations to avoid using biased handshake locations which can cause workload imbalance. Constraints (14), (15), and (16) integrate the full container flows to estimate the empty flows. Constraint (17) ensures that the number of empty flows equals the total number of loaded flows, and constraints (18) and (19) ensure that the number of loaded inbound flows equals the total number of empty outbound flows.

IV. SIMULATION OPTIMIZATION OF THE HANDSHAKE LOCATIONS UNDER DEMAND UNCERTAINTY

The SHLD provides an optimal solution under linear formulations, but may not account for dynamic impacts such as

blocking and congestion among twin OSs and vehicles in the RACT. This section describes a discrete-event simulation for the RACT and its adaptive optimization of workload balance between twin OSs under demand uncertainty.

A. DISCRETE-EVENT SIMULATION FOR THE COLLABORATIVE HANDSHAKE OPERATIONS

A large-scale material-handling system employs discrete-event simulation to evaluate and optimize operational planning. We use Siemens Tecnomatix Plant Simulation software to build the RACT simulation by referring to [2], [43], and [48]. The software provides basic objects to consider inheritance and hierarchical relationships between objects.

We modify real data on port operations and container flows from the Busan Port Terminal located in South Korea where the tasks for seaside OSs were concentrated. The seaside OSs may experience heavy workloads according to the berthing schedule. We consider the three stacking areas (SA_1, SA_2 and SA_3) handshake location candidates for loading and unloading tasks as described in Fig. 2. Each stacking area consists of 37 rows.

A cyclic operation was considered, in which the loading and unloading processes are sequentially performed [49], [50]. An OS dispatching rule widely used in real container terminals was considered, where OSs dedicatedly initiate tasks according to the origin locations of tasks to avoid heavy interference. We consider two assumptions in simulation modelling: (1) the storage capacity is sufficient for the containers to be stacked; (2) no rehandling occurs during yard operations. Fig. 5 shows the simplified discrete-event modeling of the collaborative operations.

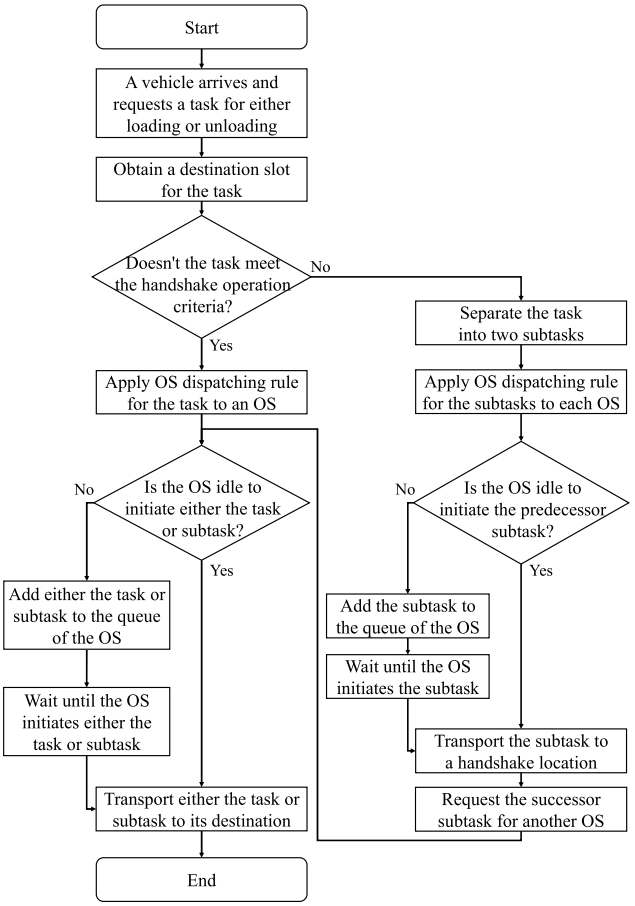

FIGURE 5. Simplified discrete-event modelling of the collaborative handshake operations.

B. BAYESIAN OPTIMIZATION FOR THE HANDSHAKE LOCATIONS

Constructing an analytical model for performance estimation can be challenging when a system exhibits uncertain and complicated behaviors with limited data. The BO iteratively estimates an objective function and recommends the most promising sample within a few observations [51]. We use the Gaussian process (GP) and expected improvement (EI) as a surrogate model and an acquisition function, respectively. GP is a non-parametric, nonlinear, flexible regression model with uncertainty quantification by inferring a stochastic process over solution space [52], [53]. A multivariate Gaussian distribution with mean and covariance functions represents the stochastic process. To determine the optimal decisions, the EI quantifies the expected improvement based on a posterior distribution.

We describe the locations for unloading and loading handshake operations using integer values, respectively. A smaller value is a nearer location to the seaside. We use a naïve rounding method that rounds the recommended continuous points to the nearest discrete points because the GP treats continuous control variables [54]. We let $x \in \mathbb{R}^2$ be a two-dimensional vector for the unloading and loading of handshake locations and $f(x)$ represent an unknown simulation output with x, where $f(x)$ is a GP denoted by the mean function $m(x)$ and covariance function $k(x, x')$:

$$f(x) \sim GP\left(m(x), k\left(x, x'\right)\right).$$

The radial basis function (RBF) the kernel function k, a widely used covariance function, expressed as

$$k\left(x_i, x_j\right) = \theta \exp\left(\frac{\left|\left|x_i - x_j\right|\right|^2}{2l^2}\right) + \sigma^2 I,$$

where the length scale parameter l adjusts the degree of smoothness, the covariance amplitude parameter θ accounts for the overall variance, and the noise term σ^2 indicates the observation noise in the posterior distribution.

Kernel matrix K denotes the covariance of the training set $D_n = \{x_{1:n}, f_{1:n}\}$, where $x_{1:n} = x_1, \ldots, x_n$ and $f_{1:n} = f(x_1), \ldots, f(x_n)$, as a multivariate Gaussian distribution. We obtain the joint distribution of $f_{1:n}$ and f_{n+1}:

$$\begin{bmatrix} f_{1:n} \\ f_{n+1} \end{bmatrix} \sim N\left(0, \begin{bmatrix} K & k \\ k^T & k\left(x_{n+1}, x_{n+1}\right) \end{bmatrix}\right),$$

where

$$K = \begin{pmatrix} k(x_1, x_1) & \cdots & k(x_1, x_n) \\ \vdots & \ddots & \vdots \\ k(x_n, x_1) & \cdots & k(x_n, x_n) \end{pmatrix} + \sigma^2 I,$$

$$k = [k(x_{n+1}, x_1), k(x_{n+1}, x_2), \ldots, k(x_{n+1}, x_n)].$$

Bayesian statistics [52] were used to derive the posterior probability distribution for x_{n+1}, expressed as follows:

$$P(f(x_{n+1}) \mid D_{1:N}) = N\left(\mu(x_{n+1}), \sigma^2(x_{n+1})\right),$$
$$\mu(x_{n+1}) = k^T K^{-1}\{y_1, \ldots, y_n\},$$
$$\sigma^2(x_{n+1}) = k(x_{n+1}, x_{n+1}) - k^T K^{-1} k.$$

EI guides the most potential point, x^*_{n+1}, toward an optimum value considering the trade-off between exploration and exploitation of a search space [55]. Exploration aims to search for x^*_{n+1} with high uncertainty, and exploitation guides x^*_{n+1} with a high expected objective value in a posterior distribution.

$$x^*_{n+1} = argmax_{x \in \chi} \mathrm{EI}_n(x).$$

The hyperparameter γ adjusts the exploration and exploitation of the search space. y^+ indicates the best solution for observations. φ and Φ are the probability and cumulative density functions, respectively, of the standard normal distribution, Z.

$$EI(x) = \begin{cases} (\mu(x) - y^+ - \gamma)\,\Phi(Z) + \sigma(x)\,\varphi(Z) & \text{if } \sigma(X) > 0 \\ 0 & \text{if } \sigma(X) = 0, \end{cases}$$

where

$$Z_n = \begin{cases} \dfrac{\mu(x) - y^+ - \gamma}{\sigma(x)} & \text{if } \sigma(X) > 0 \\ 0 & \text{if } \sigma(X) = 0 \end{cases}.$$

Fig. 6 shows the details of the proposed simulation optimization approach. We randomly set the initial values of the kernel parameters and the potential handshake locations. We optimize them via the L-BFGS-B method. From the preliminary experiments, we repeat the optimization as 50 for each iteration.

V. EXPERIMENTAL RESULTS

We vary the number of scenarios, denoted as $|S|$. Each scenario has 10 vessels. We set the nominal numbers of total tasks requested from vessels ($\overline{D_v}$) to 30, 50, and 70 for the feeder, medium, and jumbo vessels, respectively. The degree of uncertainty (π) controls the degree of demand uncertainty. We uniformly distribute the total number of tasks for vessel v in scenario s ($D_{v,s}$) in the interval $\left[\overline{D_v} \cdot (1-\pi), \overline{D_v} \cdot (1+\pi)\right]$. The detailed container flows ($f^L_s, f^U_s, f^I_s, f^O_s$) in each scenario also deviate independently and uniformly from each nominal number of tasks. We assume the same probability for each scenario.

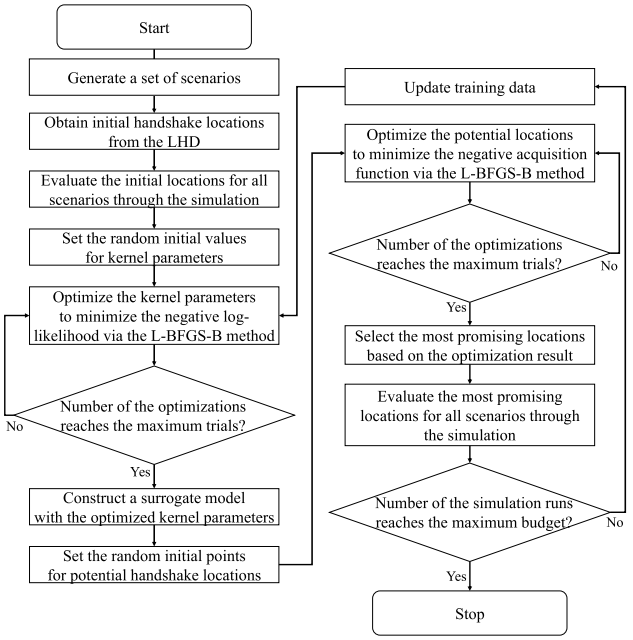

FIGURE 6. Flowchart of the proposed simulation optimization approach.

We run simulations using PC with Windows 10 Pro, Intel Core i5-10400 CPU @ 2.90 GHz, and 32 GB of RAM. We use *scikit-learn* Python library for modelling the GP and optimizing the hyperparameters in the GP.

A. COMPARATIVE RESULTS OF SIMULATION OPTIMIZATION ALTERNATIVES

A sophisticated choice of a surrogate model can speed up the simulation optimization. Latin hypercube sampling (LHS) was used to obtain 1000 data points. k-fold cross-validation ($k = 50$) was used to investigate the prediction accuracy of the GP under different levels of $|S|$ and π. Fig. 7 shows normalized root mean squared errors (nRMSEs) based on the increased amount of training data. The nRMSEs converged to 0.03 with 20 training data points for all uncertainty patterns. The results indicate that the GP can accurately predict the objective values with the different uncertainty patterns.

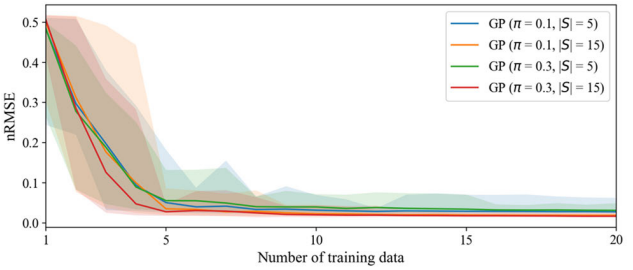

FIGURE 7. nRMSEs of the GP with the different levels of $|S|$ and π.

Next, we evaluate the convergence and efficiency of simulation optimization alternatives under different levels of $|S|$ and π. We use a scenario-based iterated local search algorithm (iLS) [56], [57], exhaustive search (ES) [3],

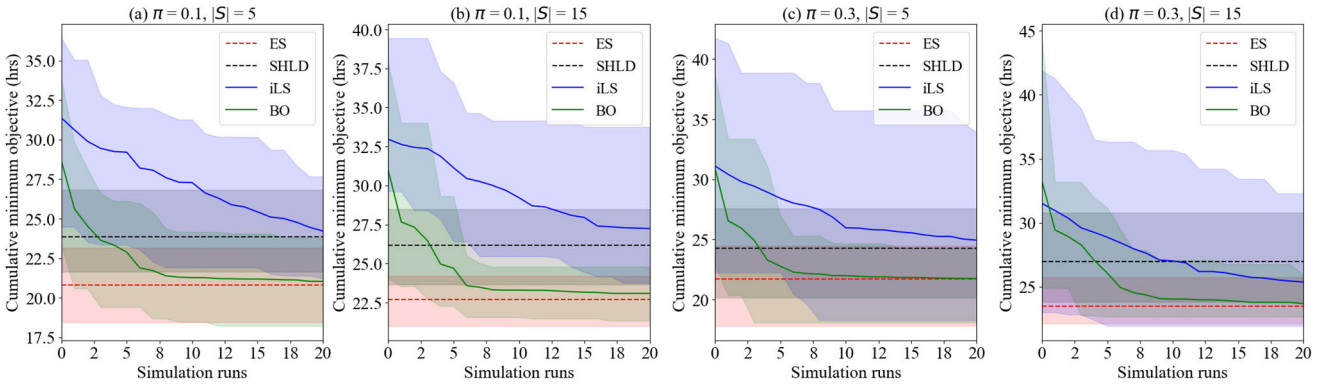

FIGURE 8. Cumulative minimum objective values of the simulation optimization alternatives for the different levels of $|S|$ and π.

[7], [15], and the SHLD as our performance benchmarks. ES conducts time-intensive simulation experiments with all candidate locations, thereby guaranteeing optimal handshake locations whereas the SHLD requires running only one simulation. The optimality gap (%) of a simulation optimization alternative is denoted as 100·(Target algorithm performance – ES performance)/(ES performance).

A cumulative minimum value is used to confirm whether a simulation optimization alternative can provide an efficient solution within a limited number of simulation runs. Fig. 8 shows the optimization performance of the four alternatives over incremented simulation runs. Each simulation optimization repeats 10 times. Since both the ES and SHLD are not adaptive approaches, there is no change in cumulative minimum values over incremented simulation runs. Fig. 8 shows performance gaps of 14.15%, 34.69%, and 11.17% for the SHLD, iLS, and BO, respectively, compared to the ES within five simulation runs, and performance gaps of 14.15%, 15.30%, and 1.07%, respectively, compared to the ES within 20 runs. The results indicate that our proposed approach yields near-optimal solutions within fewer simulation runs than the iLS.

Under the low uncertainty degree ($\pi = 0.1$), Fig 8 (a) and (b) show performance gaps of 14.91%, 18.79%, and 1.40%, respectively, for the SHLD, iLS, and BO compared to the ES. Under the high uncertainty degree ($\pi = 0.3$), Fig. 8 (c) and (d) show performance gaps of 13.38%, 11.82%, and 0.74%, respectively, for the SHLD, iLS, and BO compared to the ES. The high uncertainty increases the variations in the objective values with $|S| = 5$ from the SHLD, iLS, and BO by 37.88%, 118.88%, and 24.19%, respectively, compared to their variations under the low uncertainty, and also increases the variations with $|S| = 15$ by 25.25%, 9.27%, and 9.71%, respectively.

Computation time (simulation run time and algorithm execution time) is an important performance metric in simulation optimizations. Fig. 9 shows the computation time for each alternative. The SHLD has the shortest computing time because it only evaluates a single run, whereas the ES needs the most computation time and is the most time-consuming. The results also demonstrate that the number of scenarios proportionally increases computation time.

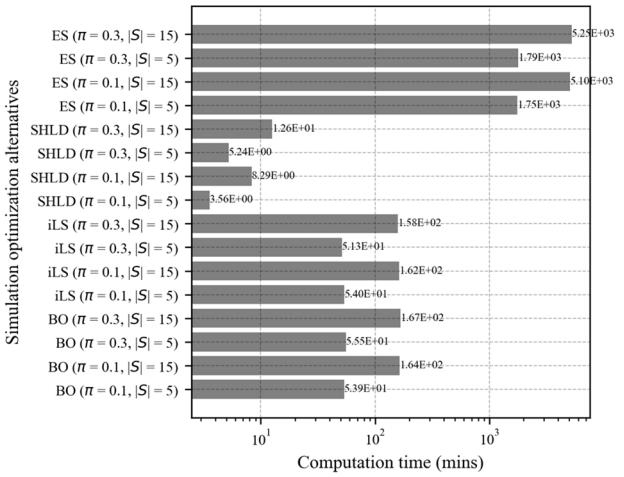

FIGURE 9. Computation time for the simulation optimization alternatives.

The average handshake locations of ten repetitions were used to validate the performance of the optimization alternatives. The maximum number of simulation runs was set to 20 because the GP's prediction accuracies showed reliable convergence (See Fig. 7). The solutions from each alternative were evaluated using 30 different maritime demands for each uncertainty pattern. Fig. 10 shows boxplots for the worst workloads of all scenarios with different π and $|S|$. The optimality gaps of the SHLD, iLS, and BO show 13.12%, 16.81%, and 0.62% for all uncertainty patterns, and BO reduces the variations in the objective values by 14.07% and 20.81% compared to the SHLD and iLS. The experimental results confirm that the BO generates near-optimal solutions and that both SHLD and iLS have relatively high optimality gaps.

Under the low uncertainty degree, the optimality gaps of the SHLD, iLS, and BO show 15.11%, 16.91%, and 1.17%, and the BO decreases the variations in the objective values by 25.40% and 21.22% compared to the SHLD and iLS. Under the high uncertainty degree, the optimality gaps of the

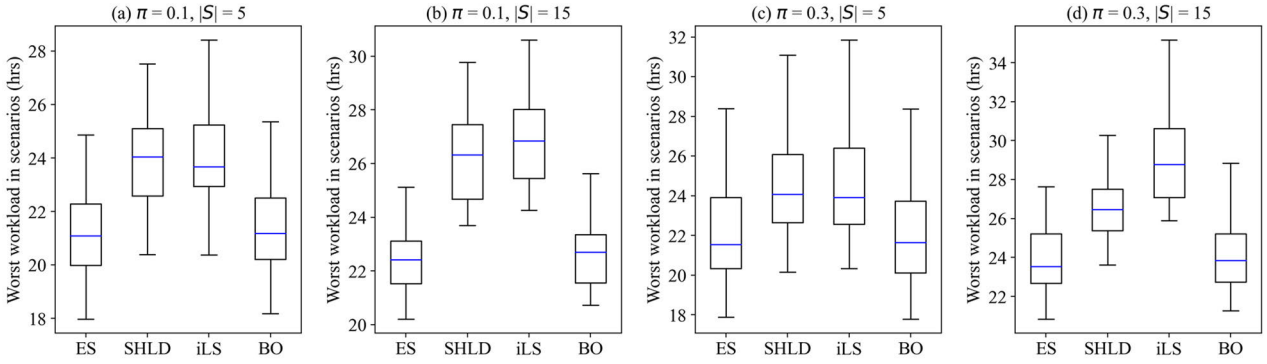

FIGURE 10. Boxplots for the worst workloads of all scenarios with the different levels of $|S|$ and π.

SHLD, iLS, and BO show 11.13%, 16.71%, and 0.07% (See Fig. 10 (c) and (d)), and the BO reduces the variations in the objective values by 2.74% and 20.39% compared to the SHLD and iLS.

To assess the robustness and effectiveness of the proposed approach with different RACT configurations, we carry out comparative experiments between the iLS and BO. Under the uncertainty pattern, $\pi = 0.1$ and $|S| = 5$, we vary the speed levels of the twin OSs, symmetrically or asymmetrically: (1) symmetric case: lower OS speed; (2) symmetric case: higher OS speed; (3) asymmetric case: lower landside OS speed; and (4) asymmetric case: lower seaside OS speed. Fig. 11 reveals that the proposed approach outperforms in the cumulative minimum objective values by 9.72%, 6.55%, 2.47%, and 17.61%, for the OS capability cases, respectively.

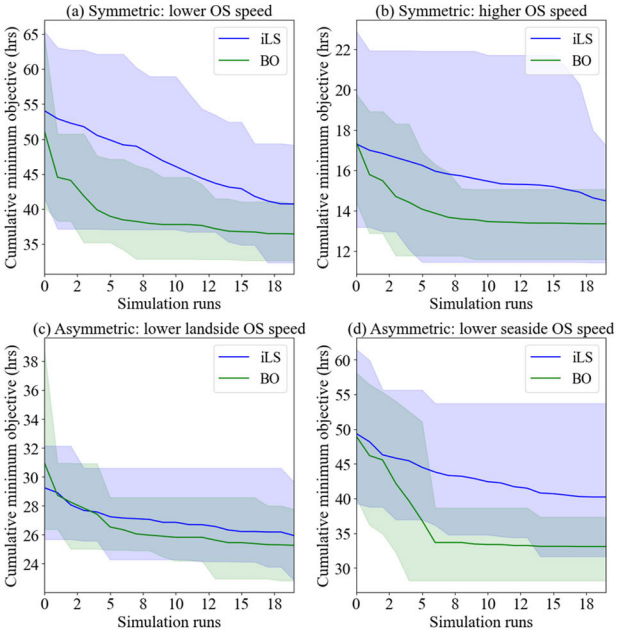

FIGURE 11. Cumulative minimum objective values of the iLS and BO for the different OS capability cases.

Fig. 11 (a) and (d) indicate that the capability degradation of the seaside OS significantly deteriorates the RACT performance.

B. SIMULATION ANALYSIS AND MANAGERIAL INSIGHTS

Allocating storage space for handshake operations is a critical issue in yard management. The required space for the handshake operations was estimated using Little's law; that is, $L = \lambda \cdot W$, where λ is the average arrival rate of subtasks, W is the average dwell time of subtasks in the handshake locations, and L is the required space for the handshake operations. We performed a simulation analysis with all possible sets of handshake locations to obtain W and λ. A simulation evaluation was performed ten times with $\pi = 0$.

Fig. 12 shows the number of slots required for loading and unloading handshake operations with the 25 location candidates closest to the seaside. Fig. 12 (a) shows significant effects of the unloading handshake location on the space required for unloading handshake operations. The unloading handshake location closer to the landside has fewer required slots because the landside OS retrieves the subtasks stacked in the handshake location as soon as the bottleneck seaside OS stores them. Fig. 12 (b) shows that the loading handshake location closer to the landside required a larger space because the bottleneck seaside OS could not quickly retrieve the subtasks in the handshake location after the landside OS stored them. The unloading handshake location closer to the landside increased the idle time of the landside OS. The landside OS utilized its idle time to transfer the subtask to be stacked at the loading handshake location. This increased the number of slots for the loading handshake operations and delayed the retrievals of the subtasks stacked in the loading handshake location owing to the workload imbalance.

Exhaustive simulations were performed to investigate the impacts of different levels of $|S|$ and π on handshake operations. Fig. 13 shows the different objective values with the different uncertainty patterns. For better visualization, the objective values with the 25 nearest location candidates to the seaside were illustrated after confirming that the optimal locations were identified close to the seaside in the

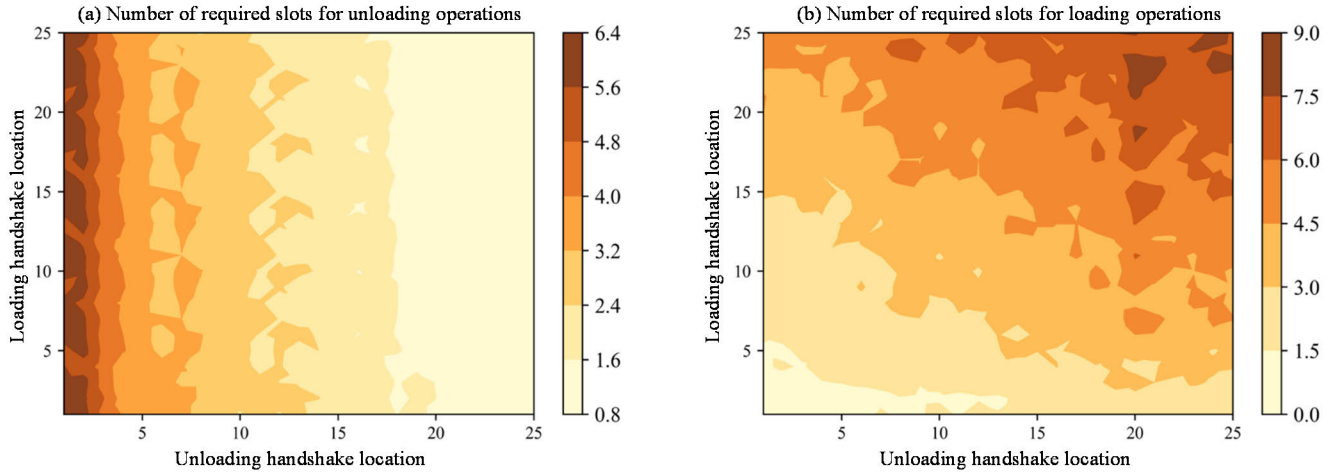

FIGURE 12. Number of required slots for the handshake operations with the different handshake locations.

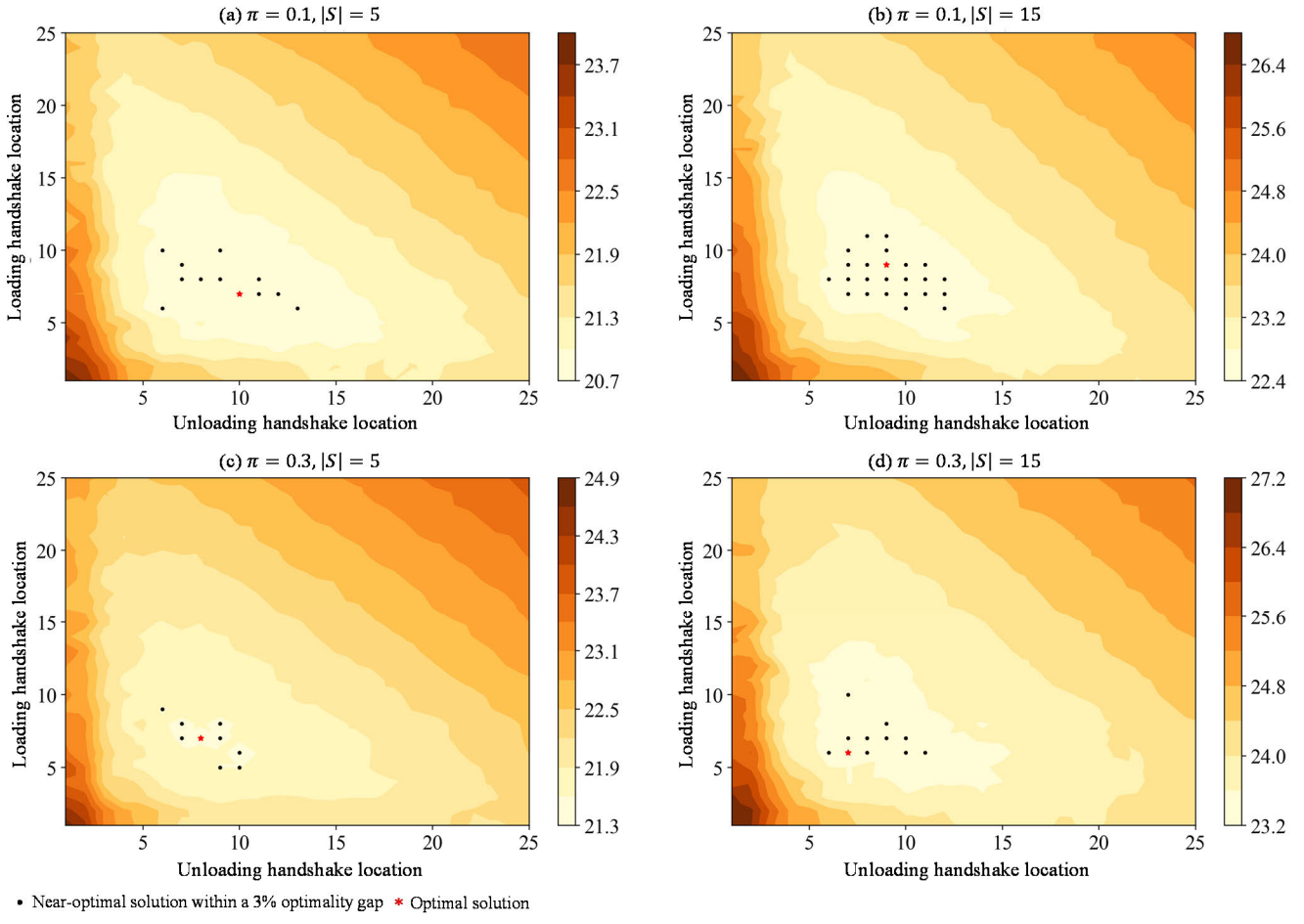

FIGURE 13. Worst workloads of all scenarios (hrs) with the different handshake locations under the different uncertainty patterns.

transshipment hub. A higher degree of uncertainty and a larger number of scenarios increase the workload of the bottleneck OS. The interference between the OSs significantly increased the objective values when the locations were biased on the seaside and landside for all uncertainty patterns. The handshake locations obtaining the near-optimal objective values within a 3% gap differ under lesser scenarios. The smaller number of scenarios with $\pi = 0.1$ showed the

sparsely distributed near-optimal solutions compared to the near-optimal solutions with the larger number of scenarios.

VI. CONCLUSION

A handshake operation aims to synchronize collaborative operations between twin transporters in a material-handling system. As a proactive optimization of yard management, a container terminal pursues reliable and effective handshake operations under maritime demand uncertainty. This study identified an MIP to clarify the scenario-based handshake location determination problem. A discrete-event simulation was built to capture time-variant and complex port operations. Extensive experiments were performed to investigate the impact of demand uncertainty on handshake operations. The simulation results indicated that the handshake location significantly influenced the space required for handshake operations and demand uncertainty is a critical factor in handshake operation for the OSs.

BO approach was also proposed to obtain efficient handshake locations within a limited number of simulations. The GP consistently identified the relationship between handshake locations and yard productivity, and the sampling schema in the BO iteratively recommended the most promising locations by controlling the trade-off between the exploration and exploitation of the solution space. The simulation results confirmed that the BO consistently provided conservative handshake operations under different demand uncertainty patterns.

We suggest the following topics for future research: (1) a full investigation of rehandling operations and inventory management issues on collaborative operations for reducing congestion in RACTs; (2) an integrated optimization of the collaborative operations of twin OSs with scheduling and routing methods for vehicles; and (3) the investigation of the handshake operations between three or more cranes in material handling systems, e.g., semiconductor fabrication plants and distribution centers. We also suggest more exploration into autonomous error detection algorithms and breakdown recovery procedures for safe operations in RACTs.

REFERENCES

[1] E. K. Lee, D. H. Jeong, and S. H. Choi, "A study on the new concept container terminal for processing containers of mega sized container ships," *J. Shipping Logistics*, vol. 30, no. 3, pp. 671–696, Sep. 2014.
[2] H. Y. Fibrianto, B. Kang, and S. Hong, "A job sequencing problem of an overhead shuttle crane in a rail-based automated container terminal," *IEEE Access*, vol. 8, pp. 156362–156377, 2020.
[3] L. Zey, D. Briskorn, and N. Boysen, "Twin-crane scheduling during seaside workload peaks with a dedicated handshake area," *J. Scheduling*, vol. 25, no. 1, pp. 3–34, Feb. 2022.
[4] X. Li, Y. Peng, J. Huang, W. Wang, and X. Song, "Simulation study on terminal layout in automated container terminals from efficiency, economic and environment perspectives," *Ocean Coastal Manage.*, vol. 213, Nov. 2021, Art. no. 105882.
[5] D. R. Dooly and H. F. Lee, "A shift-based sequencing method for twin-shuttle automated storage and retrieval systems," *IIE Trans.*, vol. 40, no. 6, pp. 586–594, Apr. 2008.
[6] Y. Kim and S. Hong, "Two picker cooperation strategies for zone picking systems with PTL technology," *IEEE Access*, vol. 8, pp. 106059–106070, 2020.
[7] X. Han, Q. Wang, and J. Huang, "Scheduling cooperative twin automated stacking cranes in automated container terminals," *Comput. Ind. Eng.*, vol. 128, pp. 553–558, Feb. 2019.
[8] A. H. Gharehgozli, F. G. Vernooij, and N. Zaerpour, "A simulation study of the performance of twin automated stacking cranes at a seaport container terminal," *Eur. J. Oper. Res.*, vol. 261, no. 1, pp. 108–128, Aug. 2017.
[9] W. Guo, M. Ji, and H. Zhu, "Multi-period coordinated optimization on berth allocation and yard assignment in container terminals based on truck route," *IEEE Access*, vol. 9, pp. 83124–83136, 2021.
[10] W. Li, S. Du, L. Zhong, and L. He, "Multiobjective scheduling for cooperative operation of multiple gantry cranes in railway area of container terminal," *IEEE Access*, vol. 10, pp. 46772–46781, 2022.
[11] R. Stahlbock and S. Voß, "Operations research at container terminals: A literature update," *OR Spectr.*, vol. 30, no. 1, pp. 1–52, Nov. 2007.
[12] J. He, W. Zhang, Y. Huang, and W. Yan, "A simulation optimization method for internal trucks sharing assignment among multiple container terminals," *Adv. Eng. Informat.*, vol. 27, no. 4, pp. 598–614, Oct. 2013.
[13] D. Chang, Z. Jiang, W. Yan, and J. He, "Integrating berth allocation and quay crane assignments," *Transp. Res. E, Logistics Transp. Rev.*, vol. 46, no. 6, pp. 975–990, Nov. 2010.
[14] B. Kang, J. Park, S. Hong, and P. V. Eko Joatiko, "Yard template planning in a transshipment hub: Gaussian process regression," in *Proc. Winter Simul. Conf. (WSC)*, Dec. 2022, pp. 1979–1989.
[15] H. Fan, W. Peng, M. Ma, and L. Yue, "Storage space allocation and twin automated stacking cranes scheduling in automated container terminals," *IEEE Trans. Intell. Transp. Syst.*, vol. 23, no. 9, pp. 14336–14348, Sep. 2022.
[16] C. Liu, X. Xiang, and L. Zheng, "A two-stage robust optimization approach for the berth allocation problem under uncertainty," *Flexible Services Manuf. J.*, vol. 32, no. 2, pp. 425–452, Jun. 2020.
[17] R. W. Bent and P. Van Hentenryck, "Scenario-based planning for partially dynamic vehicle routing with stochastic customers," *Oper. Res.*, vol. 52, no. 6, pp. 977–987, Dec. 2004.
[18] D. Briskorn, S. Emde, and N. Boysen, "Cooperative twin-crane scheduling," *Discrete Appl. Math.*, vol. 211, pp. 40–57, Oct. 2016.
[19] H. J. Carlo and F. L. Martínez-Acevedo, "Priority rules for twin automated stacking cranes that collaborate," *Comput. Ind. Eng.*, vol. 89, pp. 23–33, Nov. 2015.
[20] X. Chen, S. He, Y. Zhang, L. Tong, P. Shang, and X. Zhou, "Yard crane and AGV scheduling in automated container terminal: A multi-robot task allocation framework," *Transp. Res. C, Emerg. Technol.*, vol. 114, pp. 241–271, May 2020.
[21] F. Chu, J. He, F. Zheng, and M. Liu, "Scheduling multiple yard cranes in two adjacent container blocks with position-dependent processing times," *Comput. Ind. Eng.*, vol. 136, pp. 355–365, Oct. 2019.
[22] D.-H. Lee, H. Q. Wang, and L. Miao, "Quay crane scheduling with non-interference constraints in port container terminals," *Transp. Res. E, Logistics Transp. Rev.*, vol. 44, no. 1, pp. 124–135, Jan. 2008.
[23] L. Zhen, "Container yard template planning under uncertain maritime market," *Transp. Res. E, Logistics Transp. Rev.*, vol. 69, pp. 199–217, Sep. 2014.
[24] V. Gumuskaya, W. van Jaarsveld, R. Dijkman, P. Grefen, and A. Veenstra, "Integrating stochastic programs and decision trees in capacitated barge planning with uncertain container arrivals," *Transp. Res. C, Emerg. Technol.*, vol. 132, Nov. 2021, Art. no. 103383.
[25] T. Wang, Q. Meng, S. Wang, and X. Qu, "A two-stage stochastic nonlinear integer-programming model for slot allocation of a liner container shipping service," *Transp. Res. B, Methodol.*, vol. 150, pp. 143–160, Aug. 2021.
[26] C. Liu, X. Xiang, and L. Zheng, "Two decision models for berth allocation problem under uncertainty considering service level," *Flexible Services Manuf. J.*, vol. 29, nos. 3–4, pp. 312–344, Dec. 2017.
[27] X. Xiang and C. Liu, "An almost robust optimization model for integrated berth allocation and quay crane assignment problem," *Omega*, vol. 104, Oct. 2021, Art. no. 102455.
[28] L. Zhen, L. H. Lee, and E. P. Chew, "A decision model for berth allocation under uncertainty," *Eur. J. Oper. Res.*, vol. 212, no. 1, pp. 54–68, Jul. 2011.
[29] N. Ma, C. Zhou, and A. Stephen, "Simulation model and performance evaluation of battery-powered AGV systems in automated container terminals," *Simul. Model. Pract. Theory*, vol. 106, Jan. 2021, Art. no. 102146.
[30] M. S. Yıldırım, M. M. Aydın, and Ü. Gökkuş, "Simulation optimization of the berth allocation in a container terminal with flexible vessel priority management," *Maritime Policy Manage.*, vol. 47, no. 6, pp. 833–848, Aug. 2020.

[31] Q. Zeng, A. Diabat, and Q. Zhang, "A simulation optimization approach for solving the dual-cycling problem in container terminals," *Maritime Policy Manage.*, vol. 42, no. 8, pp. 806–826, Nov. 2015.
[32] C. Zhou, Q. Zhao, and H. Li, "Simulation optimization iteration approach on traffic integrated yard allocation problem in transshipment terminals," *Flexible Services Manuf. J.*, vol. 33, no. 3, pp. 663–688, Sep. 2021.
[33] I. Castilla-Rodrıguez, C. Expósito-Izquierdo, B. Melián-Batista, R. M. Aguilar, and J. M. Moreno-Vega, "Simulation-optimization for the management of the transshipment operations at maritime container terminals," *Expert Syst. Appl.*, vol. 139, Jan. 2020, Art. no. 112852.
[34] G. Tasoglu and G. Yildiz, "Simulated annealing based simulation optimization method for solving integrated berth allocation and quay crane scheduling problems," *Simul. Model. Pract. Theory*, vol. 97, Dec. 2019, Art. no. 101948.
[35] A. Azab, A. Karam, and A. Eltawil, "A simulation-based optimization approach for external trucks appointment scheduling in container terminals," *Int. J. Model. Simul.*, vol. 40, no. 5, pp. 321–338, Sep. 2020.
[36] S. Hong, "The effects of picker-oriented operational factors on hand-off delay in a bucket brigade order picking system," *OR Spectr.*, vol. 40, no. 3, pp. 781–808, Jul. 2018.
[37] S. Hong, "A performance evaluation of bucket brigade order picking systems: Analytical and simulation approaches," *Comput. Ind. Eng.*, vol. 135, pp. 120–131, Sep. 2019.
[38] Y. F. Lim, "Cellular bucket brigades," *Oper. Res.*, vol. 59, no. 6, pp. 1539–1545, 2011.
[39] A. Bhosekar and M. Ierapetritou, "Advances in surrogate based modeling, feasibility analysis, and optimization: A review," *Comput. Chem. Eng.*, vol. 108, pp. 250–267, Jan. 2018.
[40] A. Candelieri, R. Perego, and F. Archetti, "Bayesian optimization of pump operations in water distribution systems," *J. Global Optim.*, vol. 71, no. 1, pp. 213–235, May 2018.
[41] B. Kang, B. Kim, and S. Hong, "Sequential optimization of a temporary storage location for cooperative twin overhead shuttles in a rail-based automated container terminal," in *Proc. IFIP Int. Conf. Adv. Prod. Manage. Syst.* Cham, Switzerland: Springer, 2022, pp. 285–292.
[42] I. K. Singgih, S. Hong, and K. H. Kim, "Flow path design for automated transport systems in container terminals considering traffic congestion," *Ind. Eng. Manage. Syst.*, vol. 15, no. 1, pp. 19–31, Mar. 2016.
[43] I. K. Singgih, X. Jin, S. Hong, and K. H. Kim, "Architectural design of terminal operating system for a container terminal based on a new concept," *Ind. Eng. Manage. Syst.*, vol. 15, no. 3, pp. 278–288, Sep. 2016.
[44] S. Won, S. Cho, and S. Choi, "Operation strategies to cope with the safety accidents in overhead-shuttle container terminals," *Korean J. Logistics*, vol. 25, no. 4, pp. 33–46, Dec. 2017.
[45] S. Cho, S. Choi, and S. Won, "A study on the emergency case and management plan for a low-carbon automated container terminal," *E-Trade Rev.*, vol. 15, no. 2, pp. 93–115, 2017.
[46] C. Zhang, Y.-W. Wan, J. Liu, and R. J. Linn, "Dynamic crane deployment in container storage yards," *Transp. Res. B, Methodol.*, vol. 36, no. 6, pp. 537–555, Jul. 2002.
[47] M. C. Campi, S. Garatti, and M. Prandini, "The scenario approach for systems and control design," *Annu. Rev. Control*, vol. 33, no. 2, pp. 149–157, Dec. 2009.
[48] J. H. Seo, S. Yi, and K. H. Kim, "Dispatching vehicles in a rail-based container terminal," *J. Korean Inst. Ind. Eng.*, vol. 43, no. 6, pp. 464–473, Dec. 2017.
[49] H. Y. Bae, R. Choe, T. Park, and K. R. Ryu, "Comparison of operations of AGVs and ALVs in an automated container terminal," *J. Intell. Manuf.*, vol. 22, no. 3, pp. 413–426, Jun. 2011.
[50] V. Dhingra, D. Roy, and R. B. M. de Koster, "A cooperative quay crane-based stochastic model to estimate vessel handling time," *Flexible Services Manuf. J.*, vol. 29, no. 1, pp. 97–124, Mar. 2017.
[51] S. Greenhill, S. Rana, S. Gupta, P. Vellanki, and S. Venkatesh, "Bayesian optimization for adaptive experimental design: A review," *IEEE Access*, vol. 8, pp. 13937–13948, 2020.
[52] C. E. Rasmussen, "Gaussian processes in machine learning," in *Summer School on Machine Learning*. Cham, Switzerland: Springer, 2003, pp. 63–71.
[53] C. Park, R. Rao, P. Nikolaev, and B. Maruyama, "Gaussian process surrogate modeling under control uncertainties for yield prediction of carbon nanotube production processes," *J. Manuf. Sci. Eng.*, vol. 144, no. 3, Mar. 2022, Art. no. 031007.
[54] P. Luong, S. Gupta, D. Nguyen, S. Rana, and S. Venkatesh, "Bayesian optimization with discrete variables," in *Proc. Australas. Joint Conf. Artif. Intell.* Cham, Switzerland: Springer, 2019, pp. 473–484.
[55] D. R. Jones, M. Schonlau, and W. J. Welch, "Efficient global optimization of expensive black-box functions," *J. Global Optim.*, vol. 13, no. 4, pp. 455–492, 1998.
[56] M. Gendreau and J.-Y. Potvin, *Handbook of Metaheuristics*, 3rd ed. New York, NY, USA: Springer, 2010, pp. 363–398.
[57] S. Luke, *Essentials of Metaheuristics*, 2nd ed. Abu Dhabi, United Arab Emirates: Lulu, 2009, pp. 28–30.

BONGGWON KANG received the B.S. degree in industrial engineering from Pusan National University, South Korea, where he is currently pursuing the Ph.D. degree. His research interests include simulation modeling, analysis, and optimization of material handling operations in container terminals and semiconductor fabs.

BOSUNG KIM received the B.S. degree in industrial engineering from the Kumoh National Institute of Technology, South Korea, and the M.S. degree in industrial engineering from Pusan National University, South Korea, where he is currently pursuing the Ph.D. degree. His research interests include the optimization of material handling operations via mathematical, stochastic models, and simulation analysis.

SOONDO HONG received the B.S. and M.S. degrees in industrial engineering from POSTECH, South Korea, and the Ph.D. degree from the Department of Industrial and Systems Engineering, Texas A&M University. He has worked on scheduling, material handling, and simulation with semiconductor and display companies. He is currently a Professor with the Department of Industrial Engineering, Pusan National University, South Korea. His research interests include logistics operations, material handling, and simulation in manufacturing, warehousing, display, semiconductor, and container terminal industries. He is a member of INFORMS and the Korean Institute of Industrial Engineers.